

# On the Structures of the Hydrated Thallium(III) Ion and its Bromide Complexes in Aqueous Solution

JULIUS GLASER and GEORG JOHANSSON

Department of Inorganic Chemistry, Royal Institute of Technology (KTH), S-100 44 Stockholm, Sweden

From X-ray diffraction measurements on concentrated aqueous solutions of thallium(III) and different concentrations of bromide, the structures of the  $\text{TlBr}_n(\text{H}_2\text{O})_m^{3-n}$  ( $n=0,2,3,4$ ) complexes have been determined. The hydrated thallium(III) ion, present in acid solutions of  $\text{Tl}(\text{ClO}_4)_3$ , is shown to contain six equidistant water molecules with a Tl–O bond length of 2.235(5) Å. The second complex,  $\text{TlBr}_2^+$ , is linear with a Tl–Br distance of 2.481(2) Å and is probably associated with four water molecules leading to an octahedral species  $\text{TlBr}_2(\text{H}_2\text{O})_4^+$ . For the third complex,  $\text{TlBr}_3$ , the data are consistent with a planar triangular geometry with a Tl–Br bond length of 2.512(2) Å. Two water molecules are probably bonded to this complex, leading to a trigonal–bipyramidal  $\text{TlBr}_3(\text{H}_2\text{O})_2$  species. The  $\text{TlBr}_4^-$  complex is tetrahedral with the Tl–Br bond length 2.564(2) Å. For large bromide to thallium ratios the formation of higher species  $\text{TlBr}_n^{3-n}$  ( $n>4$ ) is indicated. Polynuclear species have not been found to be present in the solutions investigated.

The thallium(III) bromide complexes, which are among the most stable complexes known,<sup>1</sup> have been extensively investigated by several different methods.<sup>2</sup> The presence of  $\text{TlBr}^{2+}$ ,  $\text{TlBr}_2^+$ ,  $\text{TlBr}_3$ , and  $\text{TlBr}_4^-$  is well-established for dilute aqueous solutions.<sup>3–6</sup> The existence of higher species, such as  $\text{TlBr}_5^{2-}$  or  $\text{TlBr}_6^{3-}$ , has for a long time been a matter of controversy.<sup>2</sup> Thus, potentiometric,<sup>3–5</sup> solubility,<sup>4b</sup> and calorimetric measurements<sup>3,6</sup> have been interpreted to show that the formation of higher complexes is negligible. NMR measurements on concentrated aqueous solutions have been claimed to indicate that  $\text{Tl}_2\text{Br}_9^{3-}$  is the dominant species at high bromide concentrations.<sup>7</sup> A recent NMR study of the same system<sup>8</sup> has been found to

be consistent with only one higher complex formed, probably  $\text{TlBr}_6^{3-}$ , with the very small formation constant  $K_{4,6} = [\text{TlBr}_6^{3-}]/([\text{TlBr}_4^-][\text{Br}^-]^2) = 2 \times 10^{-3} \text{ M}^{-2}$ .

Very little is known about the structures of the aqua and bromide complexes of Tl(III) in solution. It has been suggested that in aqueous solutions of  $\text{Tl}(\text{ClO}_4)_3$  only two water molecules are strongly bound to  $\text{Tl}^{3+}$ .<sup>9,10</sup> For the  $\text{TlBr}_4^-$  ion Raman spectra in  $\text{CH}_2\text{Cl}_2$  and also in ethanolic and in aqueous solutions have been found to be consistent with a tetrahedral structure.<sup>11</sup>

The thallium(III) bromide complexes have well-separated regions of existence (Fig. 1). It is possible, therefore, to prepare solutions in which one single complex dominates and, since the complexes are also highly soluble, this makes them favorable for a structure determination by means of diffraction methods. The compositions of the solutions used for the present investigation are given in Fig. 1 and in Table 1. They were chosen to contain a maximal amount of each of the different complexes  $\text{TlBr}_2^+$  (in BR2),  $\text{TlBr}_3$  (in BR3),  $\text{TlBr}_4^-$  (in BR4<sub>1</sub> and BR4<sub>2</sub>), and of the hydrated metal ion (in TL1 and TL2). The  $\text{TlBr}^{2+}$  complex could not be investigated because of the spontaneous reduction of Tl(III) by the bromide ion in the corresponding solution.

The stability constants used for the calculation of the distribution of complexes in Fig. 1 were derived for the concentrations used here by a procedure described in a previous paper.<sup>8</sup>

## EXPERIMENTAL

Stock solutions were prepared and analyzed as described previously.<sup>12</sup> The compositions of the

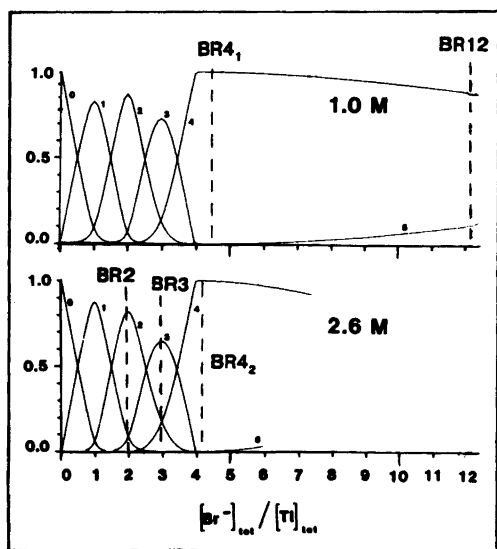


Fig. 1. Fraction of Tl(III) present as  $\text{TlBr}_n^{3-n}$  as a function of the bromide to thallium ratio (from Ref. 8) for two different total thallium concentrations. The compositions of the solutions, investigated in the present work, are indicated by the broken lines (the lines for the perchlorate solutions TL1 and TL2 coincide with the vertical axes).

solutions used for the X-ray scattering measurements are given in Table 1. The amount of Tl(I) was always less than 0.3 % of the total thallium concentration. The scattered radiation ( $\lambda_{\text{MoK}\alpha} = 0.7107 \text{ \AA}$ ) monochromatized by a focusing single crystal of lithium fluoride placed in the diffracted beam, was measured as a function of the scattering angle in a  $\theta$ - $\theta$  diffractometer described previously.<sup>13</sup> The intensities were measured at discrete points at intervals of  $0.1^\circ$  for  $1^\circ < \theta < 21^\circ$  and  $0.25^\circ$  for  $21^\circ$

$< \theta < 70^\circ$ , corresponding to the  $s$  range  $0.3 \text{ \AA}^{-1} < s = 4\pi\lambda^{-1} \sin \theta < 16.7 \text{ \AA}^{-1}$ . Typically  $10^5$  counts were accumulated for each point. A complete data collection was performed twice for each solution.

Raman spectra were recorded using a Cary 82 (Ar, 4881  $\text{\AA}$  line) and a Coderg T800 (Kr, 5682  $\text{\AA}$  line) laser spectrophotometer.

## DATA TREATMENT

After recalculation to a common slit width the intensity data were corrected for multiple scattering and polarization and were normalized to a stoichiometric unit of volume containing one Tl atom. The normalization was done by comparing observed intensities with the calculated sum of independent coherent and incoherent scattering in the high angle part of the intensity curve. The integration method<sup>14</sup> usually gave the same value for the scaling factor. Reduced intensities  $i(s)$  were calculated from the expression  $i(s) = I(s) - \sum_i n_i f_i^2(s)$ , where  $I(s)$  are the normalized observed intensities after subtraction of the incoherent scattering and  $f_i$  are the scattering factors of the atoms. The summation is taken over all atoms in the stoichiometric unit of volume.

The scattering factors for neutral atoms were taken from the International Tables for X-Ray Crystallography (1974).<sup>15</sup> Intensity contributions from water molecules were calculated using the molecular scattering factors for  $\text{H}_2\text{O}$  given by Narten *et al.*<sup>16</sup>

The incoherent scattering values were those given by Cromer *et al.*,<sup>17a</sup> Cromer<sup>17b</sup> and Compton *et al.*<sup>17c</sup> All calculations were carried out with the aid of computer programs described in a previous paper.<sup>18</sup> Radial distribution functions (RDF's),  $D(r)$  and  $D(r) - 4\pi r^2 \rho_\infty$ , were calculated with a sharpening function

Table 1. Compositions (in mol/l) of the investigated solutions.

Solution	Tl	Br	Li	H <sup>+</sup>	ClO <sub>4</sub>	H <sub>2</sub> O	Ratio Br/Tl
TL1	1.00	—	—	2.68	5.68	42.3	0
TL2	2.10	—	—	2.65	8.95	35.9	0
BR2	2.74	5.48	—	0.13	2.87	41.5	2.0
BR3	2.59	7.77	—	—	—	43.4	3.0
BR4 <sub>2</sub>	2.64	10.74	2.82	—	—	38.1	4.1
BR4 <sub>1</sub>	1.02	4.59	1.53	—	—	47.7	4.5
BR12	1.06	13.00	9.82	—	—	35.0	12.3

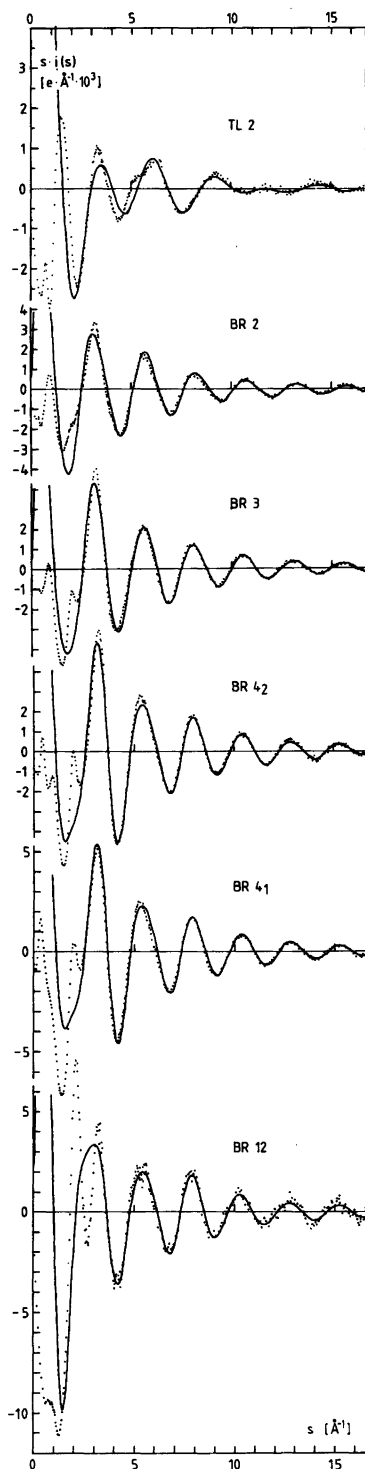


Fig. 2. Reduced intensity values,  $s \cdot i(s)$ , for the solutions investigated. Experimental values are represented by dots. Full lines show the intensities calculated for the nearest neighbour interactions shown in Fig. 3. (Note that the scale on the y-axis for the TL2 solution is expanded for clarity.)

$$M(s) = \{([n_{\text{TI}} f_{\text{TI}}(0)]^2 + [n_{\text{TI}} \Delta f_{\text{TI}}'']^2) / ([n_{\text{TI}} f_{\text{TI}}(s)]^2 + [n_{\text{TI}} \Delta f_{\text{TI}}'']^2)\} \exp(-0.007 s^2).$$

Contributions to the intensity curves from intramolecular interactions were calculated according to the expression

$$i_{\text{calc}}(s) = \sum_{\substack{p,q \\ p \neq q}} n_{pq} [f_p(s) f_q(s) + \Delta f_p'' \Delta f_q''] \frac{\sin sr_{pq}}{sr_{pq}} \cdot \exp(-\frac{1}{2} l_{pq}^2 s^2)$$

where the summation is over the atoms in the stoichiometric unit of volume and the scattering factors,  $f(s)$ , are corrected for the real part of the anomalous dispersion. Parameters characterizing intramolecular interactions, that is the distance,  $r_{pq}$ , the number of distances,  $n_{pq}$ , and the mean square variation,  $l_{pq}^2$ , were refined with a least-squares procedure, seeking the minimum for the function

$$U = \sum w(s) [i_{\text{obs}}(s) - i_{\text{calc}}(s)]^2.$$

The weighting function,  $w(s) = I^{-2}(s)$ , was chosen to give each point a weight approximately proportional to the inverse of the square of the estimated standard deviation in  $i(s)$ . In order to detect and to reduce the influence of systematic errors, the refinements were performed for different  $s$  ranges.

The  $s \cdot i(s)$  values for the solutions investigated are shown in Figs. 2 and 4 and the  $D(r) - 4\pi r^2 \rho_0$  functions in Figs. 3 and 4.

## RESULTS AND DISCUSSION

### A. The Structure of the Hydrated Thallium(III) Ion

*Intramolecular interactions.* Thallium(III) is not expected to form complexes with the perchlorate ion in aqueous solution.<sup>1,19</sup> Even in crystals of

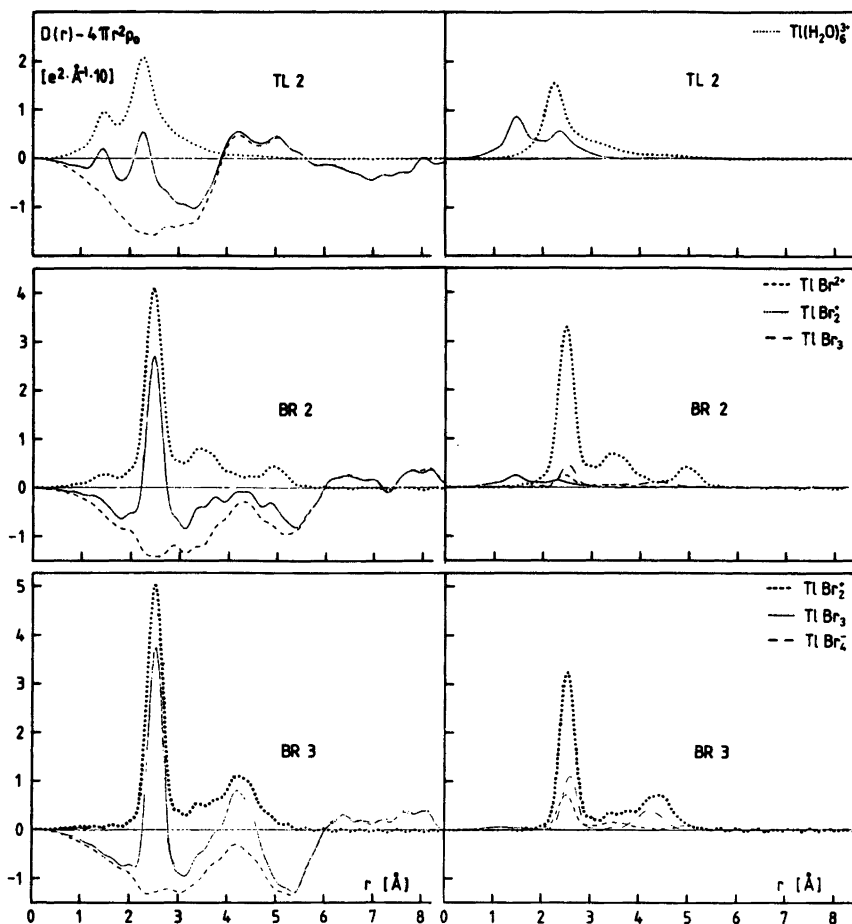


Fig. 3a. Comparison between the experimental radial distribution functions,  $D(r) - 4\pi r^2 \rho_0$ , and peak shapes, calculated for nearest neighbour interactions. The curves to the right show, for each solution, the sum of the peak shapes calculated for  $\text{H}_2\text{O}$ ,  $\text{ClO}_4^-$  and  $\text{Li}(\text{H}_2\text{O})_4^+$  (—; parameter values given in Ref. 32 were used), the sum of the peak shapes for the interactions within the dominating Tl(III) complex (···) and the corresponding contributions from the minor Tl(III) species (---).

The curves to the left represent the experimental  $D(r) - 4\pi r^2 \rho_0$  functions (—); the sum of the peak shapes shown to the right (···); and the difference between the experimental and the calculated curve (---).

$\text{Tl}(\text{ClO}_4)_3 \cdot 6\text{H}_2\text{O}$ , the  $\text{Tl}^{3+}$  ion is coordinated only to water molecules, which form a regular octahedron with  $\text{Tl}-\text{H}_2\text{O}$  bond lengths of 2.23 Å.<sup>20</sup> Perchlorate was, therefore, chosen as the anion for the determination of the structure of the hydrated thallium(III) ion in solution. The radial distribution functions for two such solutions, 1 and 2 M respectively, are shown in Fig. 4a.

The first peak in each of the RDF's occurs at about 1.4 Å and originates from the  $\text{Cl}-\text{O}$  distances within the tetrahedral perchlorate groups.<sup>21</sup> The

second peak, at about 2.3 Å, is close to the distance found for  $\text{Tl}-\text{H}_2\text{O}$  in the solid perchlorate.<sup>20</sup> Contributions to this peak should also come from the  $\text{O}-\text{O}$  distances of the perchlorate group, which are expected at about 2.3 Å. Water-water contact distances are indicated, particularly for the more dilute solution, at about 2.8 Å. The large peak between 4 and 5 Å appears differently for the two solutions and probably contains major contributions from distances between the Tl atom and molecules in its second coordination sphere.

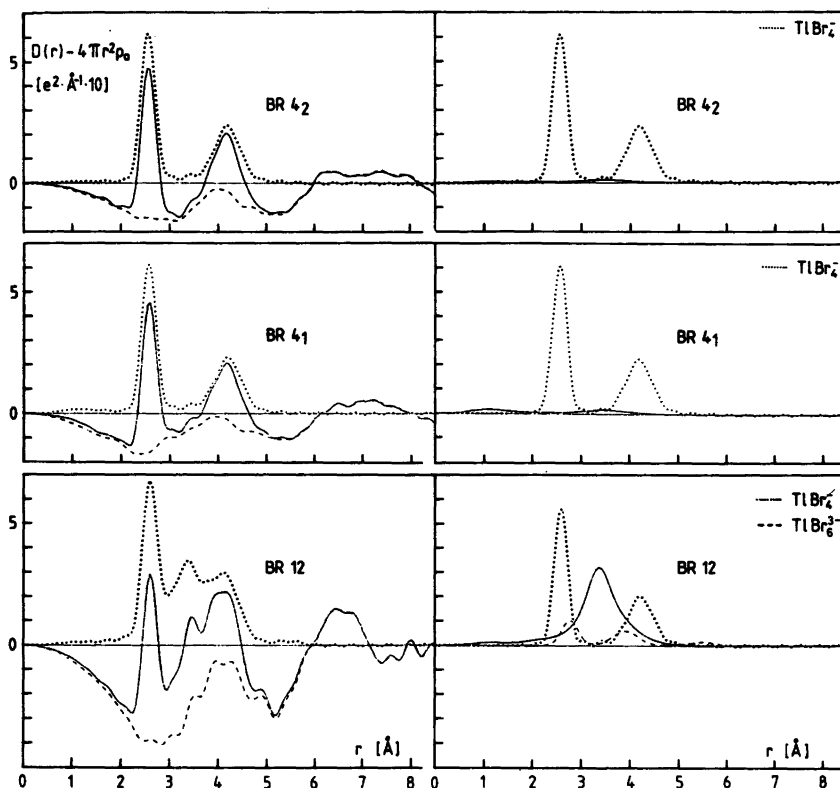


Fig. 3b. The same functions for the BR4 and the BR12 solutions as those shown for the other solutions in Fig. 3a. The vertical axes are shrunk by a factor 2 compared with those in Fig. 3a. Br-H<sub>2</sub>O contact distances<sup>32</sup> are included in the calculated peak shapes for the BR12 solution.

The well-defined intramolecular interactions of the perchlorate group and the hydrated Tl<sup>3+</sup> ion will give dominant contributions to the  $i(s)$  values in the outermost parts of the intensity curves. These parts can be used, therefore, for a least-squares refinement of the parameters characterizing the interactions. The results of a number of refinements, performed for different regions of  $s$ , are given in Table 2a. The Cl-O bond lengths are close to values found in crystal structures,<sup>21</sup> and the mean square variation,  $l_{\text{Cl-O}}^2$ , is of the same order of magnitude as the values obtained from spectroscopic measurements (0.0015 Å<sup>2</sup>).<sup>22</sup> The difference between the Cl-O bond lengths in the dilute and the concentrated solution may be significant, since it could not be traced to any systematic errors in the data. The Tl-H<sub>2</sub>O distances of 2.24 Å are identical with those found in the solid perchlorate, which indicates a similar octahedral coordination in the solution.

The number of Tl-H<sub>2</sub>O interactions per Tl atom, obtained in the least-squares refinements, is not sufficiently precise to differentiate between a fourfold and a sixfold coordination, (*cf.* Table 2a). The RDF's, however, give clear support for an octahedral coordination. This is demonstrated for example in Fig. 4b in which calculated shape functions for a thallium atom coordinating four and six water molecules, respectively, are compared with a shape function derived from the experimental RDF for the 2 M solution. This function was derived as a difference between the RDF for TL2, from which the perchlorate interactions were subtracted, and the RDF for TL1, from which the interactions within the Tl(H<sub>2</sub>O)<sub>n</sub><sup>3+</sup> ( $n=6$ ) and the ClO<sub>4</sub><sup>-</sup> units had been subtracted. The calculations were based on a stoichiometric unit of volume containing one thallium atom for the TL2 solution. For the TL1 solution, the stoichiometric volume was chosen to correspond

to the same amount of water as that for TL2. This procedure should to a large extent eliminate most of the contributions from the intermolecular interactions in the region of interest, that is around 2.3 Å.

Neither the values for the root mean square variation of the Tl–O distance obtained in the least-squares refinements nor the radial distribution

curves give any support for the occurrence of non-equivalent Tl–H<sub>2</sub>O bonds within the first coordination sphere of the Tl<sup>3+</sup> ion. It seems reasonable to assume, therefore, that the coordination of the Tl<sup>3+</sup> ion in aqueous solution is regularly octahedral, that is the same as is found in the crystals of Tl(ClO<sub>4</sub>)<sub>3</sub> · 6H<sub>2</sub>O.<sup>20</sup>

*Intermolecular interactions.* Hydrated metal ions are known to have a second coordination shell of water molecules,  $w_2$ , hydrogen bonded to the water molecules  $w_1$  of the first sphere.<sup>23</sup> In several salt hydrates the orientation of the  $w_1$  molecules can vary from mostly tetrahedral for  $M^+$  ions (a lone pair of  $w_1$  is directed towards the metal ion, while the other lone pair is accessible to accept a hydrogen bond) to usually trigonal for small  $M^{3+}$  ions ( $w_1$  points the negative side of the dipole of the H<sub>2</sub>O molecule toward the metal ion).

If the water molecules of the Tl(H<sub>2</sub>O)<sub>6</sub><sup>3+</sup> ion are assumed to be hydrogen-bonded to surrounding water molecules the corresponding Tl–H<sub>2</sub>O distances would be, assuming a  $w_1$ – $w_2$  distance of 2.75 Å, about 4.1 Å for a tetrahedral bonding, or about 4.3 Å for a trigonal arrangement. Peaks occur in the RDF's at about 4.1 Å for both the 1 M and the 2 M perchlorate solutions. In the 2 M solution, in which the number of water molecules per Tl atom is not sufficient to fill out a second coordination sphere, the 4.1 Å peak decreases and another peak occurs at 5.0 Å. This may originate from a Tl–Cl distance and may indicate an ordering of perchlorate groups within the second coordination

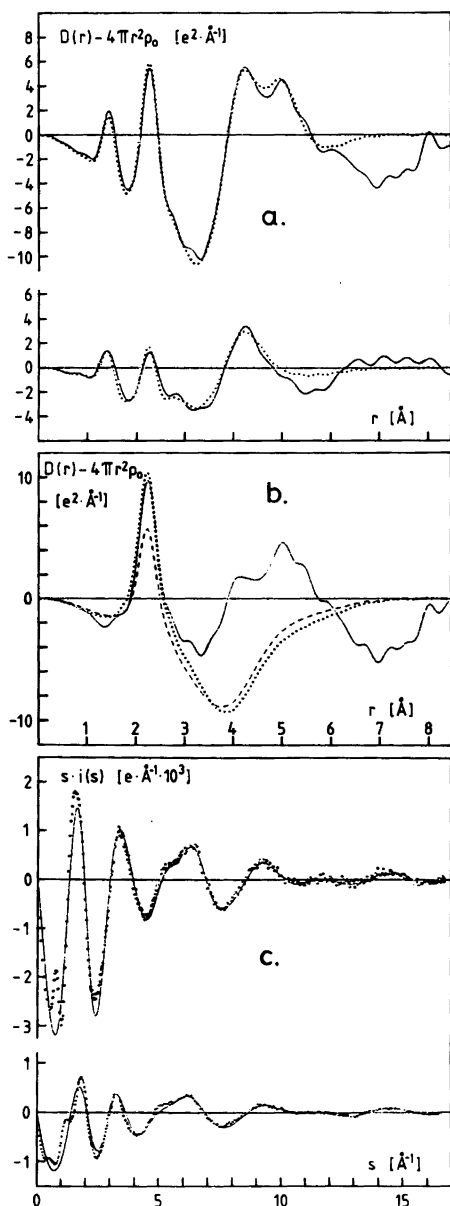


*Fig 4a.* The experimental (—) and the calculated (···) RDF's for the two Tl(III) perchlorate solutions. Intermolecular interactions have been approximated by assuming that the complexes Tl(H<sub>2</sub>O)<sub>6</sub><sup>3+</sup>, ClO<sub>4</sub><sup>-</sup> and H<sub>2</sub>O occupy spherical holes in an evenly distributed scattering density. The calculations are referred to stoichiometric units of volume containing the same number of water molecules for the two solutions. *b.* The shape function for the hydrated Tl<sup>3+</sup> ion in the TL2 solution (—) derived with the aid of the RDF for the TL1 solution. Calculated shape functions for a Tl(H<sub>2</sub>O)<sub>6</sub><sup>3+</sup> complex (···) and a Tl(H<sub>2</sub>O)<sub>4</sub><sup>3+</sup> complex (---) are given for comparison. *c.* Reduced intensity values,  $si(s)$ , for the two perchlorate solutions, referred to the same stoichiometric volumes as those in Fig. 4a. Experimental values are represented by dots. Full lines show the intensities corresponding to the theoretical curves shown in Fig. 4a.

**Table 2.** Results of least-squares refinements ( $r$  is the distance,  $n$  the number of distances per Tl atom, and  $l^2$  the mean-square variation of the distance). The estimated standard deviations are those obtained in the least-squares procedure but adjusted upwards to account for the variation in the parameters when different  $s$ -ranges were used in the refinements. Only the parameters for which standard deviations are given were refined.

Solution	$r_{\text{Tl}-(\text{H}_2\text{O})}$	$l_{\text{Tl}-(\text{H}_2\text{O})}^2$	$n_{\text{Tl}-(\text{H}_2\text{O})}$	$r_{\text{Cl}-\text{O}}$	$l_{\text{Cl}-\text{O}}^2$		
<i>a.</i> Perchlorate solutions (in $\text{ClO}_4^-$ : $l_{\text{O}-\text{O}}^2$ was held constant at $0.003 \text{ \AA}^2$ )							
TL1	2.237(5)	0.010(2)	5(1)	1.412(3)	0.0018(4)		
TL2	2.235(5)	0.008(2)	5(1)	1.443(4)	0.0046(5)		
Solution	$r_{\text{Tl}-\text{Br}}$	$l_{\text{Tl}-\text{Br}}^2$	$n_{\text{Tl}-\text{Br}}$	$r_{\text{Br}-\text{Br}}$	$l_{\text{Br}-\text{Br}}^2$	$n_{\text{Br}-\text{Br}}$	$r_{\text{Br}-\text{Br}}/r_{\text{Tl}-\text{Br}}$
<i>b.</i> Tl–Br and Br–Br interactions only (no other complexes included)							
BR2	2.485(3)	0.002(2)	1.8(2)	—	—	—	—
BR3	2.521(4)	0.006(1)	3.1(1)	4.30(2)	0.05	3(1)	1.70
BR4 <sub>2</sub>	2.563(1)	0.0038(5)	3.8(1)	4.16(3)	0.05(2)	6(1)	1.62
BR4 <sub>1</sub>	2.565(1)	0.0054(5)	4.0(1)	4.18(3)	0.05(2)	8(2)	1.63
BR12	2.593(4)	0.004(2)	4.1(3)	4.16(2)	0.05	8(2)	1.60
<i>c.</i> Tl–Br and Br–Br interactions within the main complex (the minor Tl(III) complexes included with constant parameter values)							
BR2	2.481(2)	0.004(1)	2.0	4.94(4)	0.02(2)	1.0	1.99
BR3	2.512(2)	0.004(1)	2.7(2)	4.38(5)	0.05(2)	3.0	1.74
BR4 <sub>2</sub>	2.563(1)	0.0038(5)	3.8(1)	4.16(3)	0.05(2)	6(1)	1.62
BR4 <sub>1</sub>	2.565(1)	0.0054(5)	4.0(1)	4.18(3)	0.05(2)	8(2)	1.63
BR12	2.581(4)	0.002(2)	4.0(3)	4.22(5)	0.05	7(2)	1.64

sphere. Such an ordering is also indicated by Tl–NMR measurements on aqueous solutions of  $\text{Tl}(\text{ClO}_4)_3$  in perchloric acid, where the chemical shift for the hydrated  $\text{Tl}^{3+}$  ion is clearly dependent on the concentration of the perchlorate ion.<sup>24</sup> Furthermore, in the crystal structure of  $\text{Tl}(\text{ClO}_4)_3 \cdot 6\text{H}_2\text{O}$ , the  $\text{Tl}(\text{H}_2\text{O})_6^{3+}$  unit is surrounded by fourteen  $\text{ClO}_4^-$  ions, eight of which have a Tl–Cl distance of  $5.0 \text{ \AA}$ .<sup>20</sup>

A comparison between observed and calculated  $s \cdot i(s)$  values and  $D(r) - 4\pi r^2 \rho_0$  functions for the TL1 and TL2 solutions are shown in Fig. 4. The calculated curves include contributions from intramolecular interactions of  $\text{ClO}_4^-$ ,  $\text{Tl}(\text{H}_2\text{O})_6^{3+}$ , and  $\text{H}_2\text{O}$ , and distances between Tl and molecules in an assumed second coordination sphere. Remaining intermolecular interactions are approximated by assuming that the complexes occupy spherical holes in an evenly distributed scattering density.

## B. The Structures of the Bromide Complexes

*Intramolecular interactions.* In the presence of bromide in the solutions the most pronounced

peak in the radial distribution curves appears at about  $2.5 \text{ \AA}$ , which is close to Tl–Br bonding distances found in crystal structures.<sup>25–27</sup> The second most pronounced peak is found at about  $4 \text{ \AA}$ , *i.e.* in a region where Br–Br contact distances would be expected.

The results of least-squares refinements using the high-angle parts of the intensity curves and including only the Tl–Br and the Br–Br interactions are given in Table 2b. There is a gradual increase in the Tl–Br bonding distances with the increasing Br:Tl ratio in the solutions from  $2.485(3) \text{ \AA}$  in BR2 to  $2.593(4) \text{ \AA}$  in BR12.

The number of Tl–Br interactions per Tl atom increases from 2 in the BR2 solution to 4 in the solutions containing the highest Br–Tl ratios, and thus follows the stoichiometric Br:Tl ratio except for the BR12 solution, which contains a large excess of bromide. In the two BR4 and the BR12 solutions, the ratio  $r_{\text{Br}-\text{Br}}/r_{\text{Tl}-\text{Br}}$  does not differ significantly from the theoretical value, 1.633, for a regular tetrahedral arrangement. In the solution BR3, this ratio has increased to 1.70, which indicates a larger Br–Tl–Br bonding angle in the complexes. In the solution BR2 only minor peaks appear in the region

where the Br–Br distances are expected and they were not, therefore, included in the least-squares refinement.

These results of the scattering measurements are consistent with the predictions made on the basis of the stability constants about the compositions and the distribution of the complexes in the solutions (Fig. 1). Since the stability constants were determined for the same solutions as those used for the diffraction measurements, we can, with some confidence, also use them as an estimate of the presence of minor species in each solution and introduce these as corrections in the calculations. This was done in least-squares calculations, where the Tl–Br and the Br–Br interactions within the dominating Tl(III) species in each solution were refined keeping the parameters of the minor species constant. The final results are given in Table 2c.

For the BR2 solution, the Br–Br peak is not very pronounced and other peaks, which could conceivably be taken as Br–Br intramolecular interactions, are also present (Fig. 3). The 4.94 Å peak was, however, the only one of these interactions that could be successfully refined (*cf.* Table 2c) and the most probable conclusion is, therefore, that the BR2 solution contains linear  $\text{TlBr}_2^+$  complexes ( $r_{\text{Br-Br}}/r_{\text{Tl-Br}}=2.0$ ). In the BR3 solution, the ratio found between the Br–Br and the Tl–Br distances is 1.74, which can be compared with the theoretical value of 1.732 for a planar–triangular complex. For the BR4 solutions, where the  $\text{TlBr}_4^-$  complex constitutes 99.9% of the total thallium content, according to the stability constants, the results are, of course, identical with those given in Table 2b. The BR12 solution will be discussed below.

*Comparison with crystal structures and spectroscopic measurements.* It is of interest to compare the structures of the complexes, derived from the solution scattering data, with those found in the solid state. Unfortunately, no crystals with a stoichiometric Br/Tl ratio of 2:1 are known and no  $\text{TlBr}_2^+$  complexes have yet been found in any crystal structure. Crystals of  $\text{TlBr}_3 \cdot 4\text{H}_2\text{O}$  contain almost planar triangular  $\text{TlBr}_3$  complexes with Tl–Br bonding distances of 2.515(3) Å,<sup>25</sup> the same as those found for the solution BR3 (Table 2c). In the crystal structure, the Tl atom is also in contact with two water molecules at distances of 2.60(2) and 2.52(2) Å, respectively, thus forming a trigonally bipyramidal arrangement. In the radial distribution function for the BR3 solution no separate peaks corresponding to such Tl–H<sub>2</sub>O distances can be distinguished but

they have been assumed to be present for the calculation of the peak shapes (Fig. 3). The Tl–NMR chemical shift for the third complex in aqueous solution is close to the shift for the compound  $\text{TlBr}_3 \cdot 4\text{H}_2\text{O}$ .<sup>8</sup> This is in agreement with the assumption, that the essentially trigonal–bipyramidal  $\text{TlBr}_3(\text{H}_2\text{O})_2$  complex found in the solid is also present in the solution.

Tetrahedral  $\text{TlBr}_4^-$  units occur in crystals of  $\text{KTlBr}_4 \cdot 2\text{H}_2\text{O}$ .<sup>26b</sup> The Tl–Br distances of 2.554(3) Å do not differ significantly from those found in the solution, 2.564(2) Å (Table 2c). Discrete  $\text{Tl}_2\text{Br}_9^{3-}$  ions, consisting of two face-sharing  $\text{TlBr}_6$  octahedra, probably occur in crystals of  $\text{Cs}_3\text{Tl}_2\text{Br}_9$ ,<sup>8,12</sup> and have been proposed to be the dominant species in concentrated aqueous solutions with high Br:Tl ratios.<sup>7</sup> The scattering data for the 2.6 M solution BR4<sub>2</sub> and the 1 M solutions BR4<sub>1</sub> and BR12 give no support for this assumption. Nor could any support be obtained from the Tl–NMR measurements.<sup>8</sup>

Preliminary results for a crystal structure determination of  $\text{Rb}_3\text{TlBr}_6 \cdot \frac{13}{7}\text{H}_2\text{O}$  show that it contains octahedral  $\text{TlBr}_6^{3-}$  units with Tl–Br distances of about 2.75 Å.<sup>12</sup> NMR measurements on aqueous solutions<sup>8</sup> have indicated that for very large Br:Tl ratios, higher complexes than  $\text{TlBr}_4^-$  can form, probably  $\text{TlBr}_6^{3-}$  (Fig. 1). With the stability constants derived from the NMR measurements, we can estimate that in the BR12 solution the concentration of the  $\text{TlBr}_6^{3-}$  complex would amount to about 13% of the total thallium content. The resulting change in the number of the Tl–Br interactions from that expected for  $\text{TlBr}_4^-$  complexes alone would be below the significance level in our determinations (Table 2b). The expected change in the Tl–Br distance would, however, if estimated as a weighted average between the distances in the  $\text{TlBr}_4^-$  and the  $\text{TlBr}_6^{3-}$  complexes, be around 0.035 Å and should be observable. The least-squares refinements show an increase in the Tl–Br distance for the BR12 solution of 0.03 Å compared with that found for the BR4<sub>1</sub> solution (Table 2b), and this is probably a significant difference. It may support the assumption of the formation of a higher complex than  $\text{TlBr}_4^-$ , although other explanations of this difference are possible, especially when the rather drastic changes in composition between the BR4 and the BR12 solutions are considered (see below).

Results from Raman measurements are consistent with these conclusions as far as the higher complexes



are concerned. Spectra for the BR4<sub>1</sub> solution and for a 3.2 M solution with a Br/Tl ratio of 4.5 do not differ significantly and the frequencies observed (~200 sh, 187 vs, ~57 w) are in agreement with those for crystals containing tetrahedral TlBr<sub>4</sub><sup>-</sup> units (e.g. KTlBr<sub>4</sub>·2H<sub>2</sub>O<sup>28</sup>) and for the, presumably, tetrahedral TlBr<sub>4</sub><sup>-</sup> complexes present in the noncoordinating solvents CH<sub>3</sub>CN<sup>29</sup> and CH<sub>2</sub>Cl<sub>2</sub>.<sup>11b</sup> If Tl<sub>2</sub>Br<sub>9</sub><sup>3-</sup> species were present in the solutions, much more complex spectra would be expected, as judged from the Raman spectrum of the compound Cs<sub>3</sub>Tl<sub>2</sub>Br<sub>9</sub> (206 m, 192 s, 186 vs, 159 vs, 139 w, 96 w, 69 m etc.).

The BR12 solution gives the same Raman spectrum as that for the BR4<sub>1</sub> solution except for a small but significant frequency shift of the Tl–Br symmetric stretching line from 185.7 cm<sup>-1</sup> to 184.5 cm<sup>-1</sup>. This indicates a weakening of the Tl–Br bonds and probably corresponds to a lengthening of these bonds. The Raman measurements of Jones, who investigated the dependence of the Hg–Cl frequencies on the Hg–Cl bond length,<sup>30</sup> would suggest that a drop of 1.2 cm<sup>-1</sup> as observed here corresponds to a bond lengthening of about 0.005 Å. This cannot explain the difference of 0.03 Å between the Tl–Br distances obtained in the least-squares refinements for the BR4<sub>1</sub> and the BR12 solutions (Table 2b) and thus it supports the conclusion that this difference results from the formation of higher complexes, probably TlBr<sub>6</sub><sup>3-</sup>. Raman lines for a TlBr<sub>6</sub><sup>3-</sup> complex are probably too weak to be observed in the BR12 solution. Their expected positions can be inferred from the Raman spectrum of the compound [Co(NH<sub>3</sub>)<sub>6</sub>]TlBr<sub>6</sub> containing octahedral TlBr<sub>6</sub><sup>3-</sup> units<sup>27</sup> (160 vs, 89 m, 72 w, 56 w, 39 m, 27 s).

*Intermolecular interactions.* A comparison of the observed  $D(r) - 4\pi r^2 \rho_0$  functions with calculated peak shapes, based on the parameter values in Table 2c and the distribution of complexes according to Fig 1, is shown in Fig. 3. Subtraction of the calculated peaks leads, for all of the bromide solutions, to smooth background curves with remaining diffuse maxima primarily in the region between 3 and 5 Å, where H<sub>2</sub>O–H<sub>2</sub>O (2.8 Å), Br–H<sub>2</sub>O (3.3 Å) and distances between the Tl atom and molecules in its second coordination sphere are expected.

For the BR4<sub>1</sub> solution, which contains almost solely tetrahedral TlBr<sub>4</sub><sup>-</sup> complexes and Li<sup>+</sup> ions, probably as tetrahedral Li(H<sub>2</sub>O)<sub>4</sub><sup>+</sup>,<sup>32</sup> a simple model for the approximation of the intermolecular interactions was employed. A packing of water molecules around the TlBr<sub>4</sub><sup>-</sup> complex, as illustrated in Fig. 5 and previously used for solutions containing HgBr<sub>4</sub><sup>-</sup> complexes,<sup>31</sup> with a continuous electron distribution outside a sphere of radius 5 Å leads to a good agreement between observed and calculated  $si(s)$  values even in the low angle region of the intensity curve as shown in Fig. 6. In this figure, the  $D(r)$  function, calculated with the aid of this model, is also compared with the experimental function.

## CONCLUSIONS

The results obtained with the different methods discussed above are all consistent and lead to the following overall picture of the complex formation between Tl(III) and Br<sup>-</sup> in aqueous solution. In solutions of thallium(III) perchlorate, thallium is octahedrally surrounded by six equidistant water molecules with Tl–O bond lengths of 2.235(5) Å.

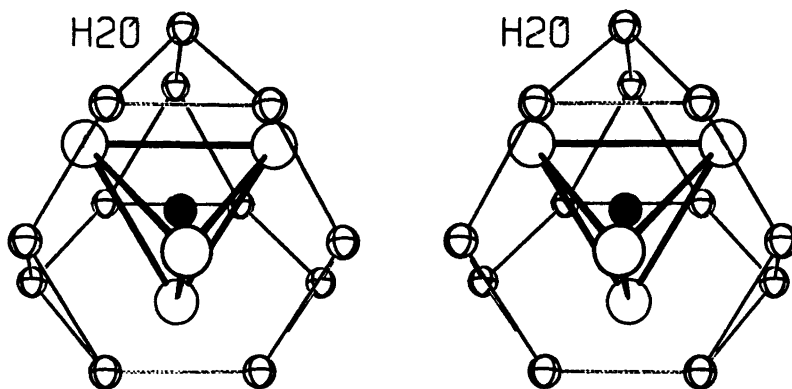


Fig. 5. The model used in the calculations for the packing of water molecules around the TlBr<sub>4</sub><sup>-</sup> complex.

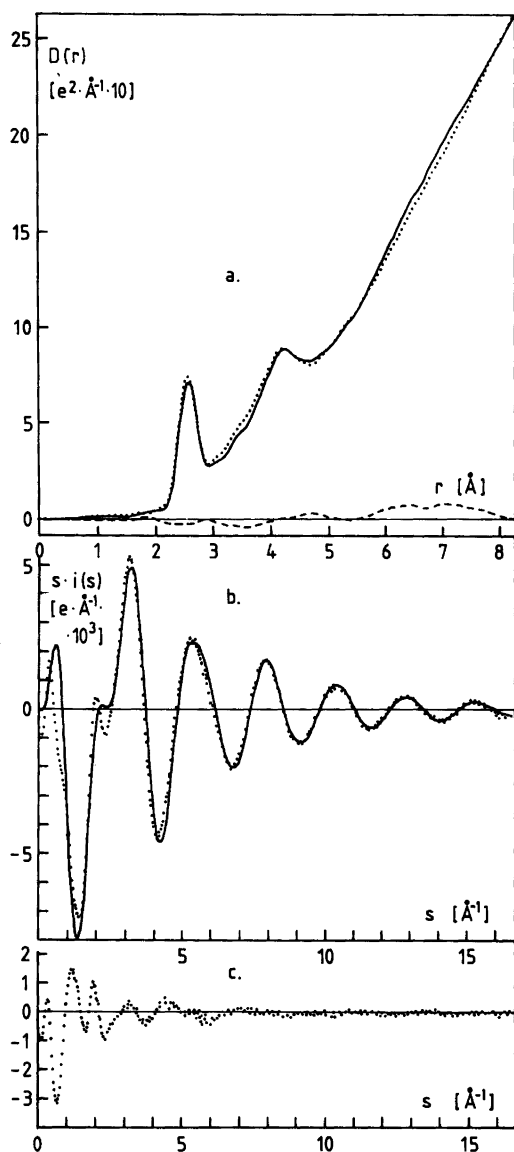


Fig. 6a. Comparison between the experimental RDF for the BR<sub>4</sub><sub>1</sub> solution (—) and a calculated function including both intra- and intermolecular interactions (···). The difference between the experimental and the calculated curve is given by the broken line.

b. Comparison of the experimental  $si(s)$  curve (···) with the curve calculated for the model shown in Fig. 6a (—). c. The difference between the experimental and the calculated  $si(s)$  curves shown in Fig. 6b.

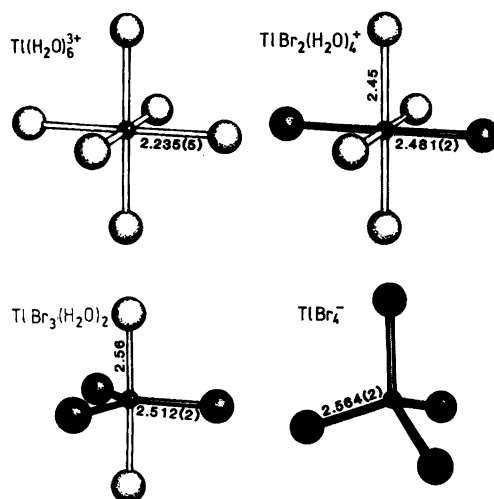


Fig. 7. Suggested structures for the  $TiBr_n(H_2O)_m^{3-n}$  complexes in aqueous solution. Only the distances for which standard deviations are given have been determined. Dark spheres represent Br and light spheres  $H_2O$ .

When bromide is added, the octahedral symmetry is retained in the first two complexes formed,  $TiBr_2^{+}$  and  $TiBr_3$ , which results in a linear  $TiBr_2^{+}$  complex with  $Ti-Br$  distances of 2.481(2) Å. When the third complex,  $TiBr_3$ , is formed, the coordination changes to trigonal-planar with  $Ti-Br$  distances of 2.512(2) Å. The fourth complex,  $TiBr_4^{-}$ , has as regular tetrahedral symmetry with  $Ti-Br$  bond lengths of 2.564(2) Å. For very large  $Br/Ti$  ratios small amounts of a higher complex form, probably an octahedral  $TiBr_6^{3-}$  species. The structures of the complexes are illustrated in Fig. 7. A comparison between the calculated peak shapes and the experimental RDF's (Fig. 3), as well as the good agreement between calculated and experimental intensity values at high  $s$  ranges (Fig. 2) confirm the conclusions made on the structures of the complexes.

*Acknowledgements.* We thank Dr. Peter Goggin and Dr. Magnus Sandström for recording the Raman spectra and Mr. Ernst Hansen for skilful technical assistance.

The work has been supported by the Swedish Natural Science Research Council (NFR).

## REFERENCES

1. a. Smith, R. M. and Martell, A. E. *Critical Stability Constants*, Plenum, New York 1977, Vol. 4; b. Sillén, L. G. and Martell, A. E. *Stability Constants*, The Chemical Society, London 1964.
2. Lee, A. G. *The Chemistry of Thallium*, Elsevier, Amsterdam 1971 and references therein.
3. Woods, M. J. M., Gallagher, P. K., Hugus, Z. Z. and King, E. L. *Inorg. Chem.* 3 (1964) 1313.
4. a. Ahrland, S., Grenthe, I., Johansson, L. and Norén, B. *Acta Chem. Scand.* 17 (1963) 1567; b. Ahrland, S. and Johansson, L. *Acta Chem. Scand.* 18 (1964) 2125.
5. Yakovlev, Y. B., Kulba, F. Y. and Mironov, V. E. *Zh. Neorg. Khim.* 12 (1967) 3283.
6. Leden, I. and Ryhl, T. *Acta Chem. Scand.* 18 (1964) 1196.
7. Figgis, B. N. *Trans. Faraday Soc.* 55 (1959) 1075.
8. Glaser, J. and Henriksson, U. *J. Am. Chem. Soc.* 103 (1981) 6642.
9. Biedermann, G. and Spiro, T. G. *Chem. Scr.* 1 (1971) 155.
10. Spiro, T. G. *Inorg. Chem.* 4 (1965) 731.
11. a. Delwaulle, M. L. *C. R. Acad. Sci. Fr.* 238 (1954) 2522; b. Andrews, S. P., Badger, P. E. R., Goggin, P. L., Hurst, N. W. and Ratray, A. J. M. *J. Chem. Res. (M)* (1978) 1401; c. Davies, E. D. and Long, D. A. *J. Chem. Soc. A* (1968) 2050.
12. Glaser, J. *Thesis*, Royal Institute of Technology, Stockholm 1981.
13. Johansson, G. *Acta Chem. Scand.* 20 (1966) 553.
14. a. Norman, N. *Thesis* Na 219 (1954) Universitetets Fysiska Institut, Oslo; *Acta Crystallogr.* 10 (1957) 370; b. Krogh-Moe, J. *Acta Crystallogr.* 9 (1956) 951.
15. *International Tables for X-Ray Crystallography*, Kynoch Press, Birmingham 1974, Vol. IV.
16. Narten, A. H. and Levy, H. A. *J. Chem. Phys.* 55 (1971) 2263.
17. a. Cromer, D. T. and Mann, J. B. *J. Chem. Phys.* 47 (1967) 1892; b. Cromer, D. T. *J. Chem. Phys.* 50 (1969) 4857; c. Compton, A. H. and Allison, S. K. *X-Rays in Theory and Experiment*, Van Nostrand, New York 1935.
18. Johansson, G. and Sandström, M. *Chem. Scr.* 4 (1973) 195.
19. Hester, R. E. *Inorg. Chem.* 3 (1964) 769.
20. Glaser, J. and Johansson, G. *Acta Chem. Scand.* A 35 (1981) 639.
21. Berglund, B., Thomas, J. O. and Tellgren, R. *Acta Crystallogr. B* 31 (1975) 1842.
22. a. Nagarajan, G. *Indian J. Pure Appl. Phys.* 2 (1964) 17; b. Müller, A. and Nagarajan, G. *Z. Naturforsch. Teil. B* 21 (1966) 508.
23. Friedman, H. L. and Lewis, L. *J. Sol. Chem.* 5 (1976) 445.
24. *Unpublished results* from this laboratory.
25. a. Zvonkova, Z. V. *Zh. Fiz. Khim.* 30 (1956) 340; b. Glaser, J. *Acta Chem. Scand. A* 33 (1979) 789.
26. a. Hazell, A. C. *J. Chem. Soc.* (1963) 3459; b. Glaser, J. *Acta Chem. Scand. A* 34 (1980) 157.
27. Watanabe, T., Atoji, M. and Okazaki, Ch. *Acta Crystallogr.* 3 (1950) 405.
28. Spiro, T. G. *Inorg. Chem.* 6 (1967) 569.
29. Walton, R. A. *Coord. Chem. Rev.* 6 (1971) 1.
30. Jones, T. *Thesis*, City Polytechnic, Sheffield 1979.
31. Sandström, M. and Johansson, G. *Acta Chem. Scand. A* 31 (1977) 132.
32. a. Palinkas, G., Radnai, T. and Hajdu, F. *Z. Naturforsch. Teil. A* 35 (1980) 107; b. Narten, A. H., Vaslov, F. and Levy, H. A. *J. Chem. Phys.* 58 (1973) 5017.

Received May 22, 1981.